

# First principles lattice dynamics of NaCoO<sub>2</sub>

Zhenyu Li, Jinlong Yang,\* J.G. Hou, and Qingshi Zhu

*Laboratory of Bond Selective Chemistry and Structure Research Laboratory,  
University of Science and Technology of China, Hefei, Anhui 230026, P.R. China*

(Dated: November 11, 2018)

## Abstract

We report first principles linear response calculations on NaCoO<sub>2</sub>. Phonon frequencies and eigenvectors are obtained throughout the Brillouin zone for two geometries with different Na site occupancies. While most of the phonon modes are found to be unsensitive to the Na site occupancy, there are two modes dominated by out-of-plane vibrations of Na giving very different frequencies for different geometries. One of these two modes, the A<sub>2u</sub> mode, is infrared-active, and can be used as a suitable sensor of Na distribution/ordering. The longitudinal-transverse splitting of the zone-center optical-mode frequencies, Born effective charges and the dielectric constants are also reported, showing considerable anisotropy. The calculated frequencies of Raman-active modes generally agree with the experimental values of corresponding Na de-intercalated and/or hydrated compounds, while it requires better experimental data to clarify the infrared-active mode frequencies.

PACS numbers: 63.20.Dj, 71.20.Ps, 74.25.Kc

## I. INTRODUCTION

Since the discovery of the superconductivity in  $\text{Na}_x\text{CoO}_2 \cdot y\text{H}_2\text{O}$ ,<sup>1</sup> significant interest has been focused on this novel material, because there are some intriguing similarities between this cobalt oxide superconductor and copper oxide superconductors.<sup>2</sup> A number of evidences in experiments suggest that the superconductivity in this material is unconventional.<sup>3,4,5</sup> Theoretical models such as resonating valence bond (RVB)<sup>6,7,8,9</sup> and spin-triplet superconductivity<sup>10,11,12,13</sup> with strong magnetic quantum fluctuations are also proposed. Although now it is a consensus that the cobalt oxide superconductor is not simply a BCS superconductor, some experiments still suggest the possible strong lattice coupling to the electronic density of states in this compound.<sup>14,15</sup> It is thus important to fully characterize the lattice dynamical properties of  $\text{Na}_x\text{CoO}_2 \cdot y\text{H}_2\text{O}$  and related materials.

While there are some Raman,<sup>16,17</sup> infrared,<sup>14,18</sup> and neutron scattering<sup>19</sup> experiments involving the lattice dynamics of the cobalt oxide compound, there is no first principles theoretical report found in the literature. In this article, we report a density functional perturbation theory (DFPT)<sup>20,21</sup> calculation on  $\text{NaCoO}_2$ , the intrinsic (without hydration or de-intercalation of Na) insulating phase of the cobalt oxide superconductor. As shown in Figures 1a and 1b,  $\text{NaCoO}_2$  has a hexagonal structure (space group #194,  $\text{P6}_3/\text{mmc}$ ) consisting of  $\text{CoO}_2$  layers of edge sharing  $\text{CoO}_6$  octahedra and Na layers with two partly occupied Na Wyckoff sites. To accommodate for the partial occupation of the two Na sites, we consider two geometries of  $\text{NaCoO}_2$  with one site fully occupied and the other site empty, namely geometry *A* (Figure 1a) with the  $2b$  site occupied and geometry *B* (Figure 1b) with the  $2d$  site occupied.

## II. COMPUTATIONAL METHOD

The present results have been obtained through the use of the ABINIT code,<sup>22</sup> a common project of the Universit Catholique de Louvain, Corning Incorporated, and other contributors (URL <http://www.abinit.org>), based on pseudopotentials and plane waves. It relies on an efficient fast Fourier transform algorithm for the conversion of wave functions between real and reciprocal spaces, on the adaptation to a fixed potential of the band-by-band conjugate gradient method<sup>23</sup>, and on a potential-based conjugate-gradient algorithm for the

determination of the self-consistent potential.<sup>24</sup> Technical details on the computation of responses to atomic displacements and homogeneous electric fields can be found in Ref. 21, and the subsequent computation of dynamical matrices, Born effective charges, dielectric permittivity tensors, and interatomic force constants was described in Ref. 25.

Troullier-Martins norm conserving pseudopotentials<sup>26</sup> are used, with Teter parametrization<sup>27</sup> of the Ceperley-Alder exchange-correlation potential. The kinetic energy cutoff of the plane wave bases is 50 hartree. A uniform  $6\times 6\times 2$   $k$ -point mesh is used in Brillouin-zone integrations, which gives well converged total energies and phonon frequencies.

### III. RESULTS AND DISCUSSION

#### A. Geometries and Electronic Structures

As a first step, we optimize the geometry and calculate the corresponding electronic structure. During the geometry optimization, the cell parameters are fixed to the experimental values of  $\text{Na}_{0.74}\text{CoO}_2$  ( $a = 2.84\text{\AA}$ ,  $c = 10.811\text{\AA}$ ).<sup>28</sup> We notice that neutron scattering experiments<sup>28,29,30</sup> for samples with different Na concentrations give similar cell parameters. Considering the space group symmetry, the only freedom to be relaxed is the Co-O layer space  $d$ , which turns out to be 1.897 and 1.899  $\text{\AA}$  for geometries  $A$  and  $B$  respectively. The electronic band structure and density of states (DOS) based on the optimized structure of geometry  $A$  are shown in Figure 1c, a gap of 0.94 eV (from 0.60 to 1.54 eV) between the valence band and the conduction band can be clearly identified. Little difference on the electronic structure of the two geometries is found. This similarity strongly indicates that Na contributes to the electronic structure only by doping electrons to the CoO layers.

#### B. Phonon Dispersions

To map the phonon dispersion curves throughout the Brillouin zone, the dynamical matrices are obtained on a uniform  $6\times 6\times 2$  grid of  $q$  points, and real-space force constants are then found by Fourier transform of the dynamical matrices. The dynamical matrix at an arbitrary wave vector  $\mathbf{q}$  can then be computed by an inverse Fourier transform. The acoustic sum rule is applied to force the three acoustic phonon frequencies at  $\Gamma$  equal to zero

strictly as being implied by the translation symmetry. The calculated phonon dispersions and corresponding DOS for geometries *A* and *B* are shown in Figure 2. We see first that both structures are stable. Second, we notice that the phonon modes are separated to two groups in frequency, namely the soft group with frequencies below than about  $400 \text{ cm}^{-1}$  and the hard group with frequencies between  $450$  to  $650 \text{ cm}^{-1}$ . As a whole, the phonon dispersions for the two geometries with different Na site occupancies are similar, but there are also some minor differences exist for the two geometries in the phonon band structure, unlike the nearly identical electronic band structures. First, as we will discussed in detail below, there are some soft modes giving significant different frequencies near zone center for the two geometries. Secondly, we notice that the dispersion along  $\Gamma - A$  for geometry *B* is larger than that for geometry *A*.

### C. zone-center phonon modes

The zone-center phonon modes are of special importance, since they can be obtained by various of experimental methods. In Table I, we list the frequencies, symmetries and vibration modes of the zone-center phonons. The triply-degenerated acoustic mode with zero frequency is not listed. The frequency differences between the two geometries are generally small, especially for the Raman-active phonon modes. However there are an infrared-active  $A_{2u}$  mode and a silent  $B_{1g}$  mode giving very different frequencies for geometry *A* and geometry *B*, and both of these two modes are mainly contributed by the Na out-of-plane vibrations. The other  $A_{2u}$  and  $B_{1g}$  modes (modes 7 and 14) also involve the out-of-plane vibrations of Na, but we notice that the vibrations of Co and/or O in these two modes are much stronger than or at least comparable to the Na vibrations. Therefore they give relatively small frequency differences for different Na site occupancies. We find that the frequency difference of Raman-active  $A_{1g}$  mode of O out-of-plane vibrations is rather small, in contrast to the conclusion of the shell model calculations by Lemmens et al..<sup>17</sup> They found a pronounced frequency dependence of the  $A_{1g}$  mode, and argued that it would be used as a very susceptible sensor of Na distribution/ordering. However, in our first principles calculations, the infrared-active  $A_{2u}$  mode (mode 6) in the soft group may be more suitable to act as the sensor mode. Another difference between  $\Gamma$  phonon modes of the two geometries is the frequency order of the first  $E_{2g}$  and  $B_{2u}$  modes (modes 1 and 10).

Since the systems we studied here are polar materials, we also get the longitudinal-transverse optical mode (LO-TO) splittings by considering response to the macroscopic electric field. As shown in Table I, the LO-TO splittings are found only in the infrared-active  $2E_{1u} + 2A_{2u}$  modes. The biggest LO-TO splitting is found in the hard  $E_{1u}$  mode, with  $\Delta\omega = \omega_{LO} - \omega_{TO}$  equal to 52.4 and 48.6  $\text{cm}^{-1}$  for geometries *A* and *B* respectively. Contrastingly, the soft  $E_{1u}$  mode is split by only 5.1 and 5.9  $\text{cm}^{-1}$  respectively. Both these two  $E_{1u}$  modes are "layer sliding" modes, and the hard one is mainly contributed by the Co layers sliding against the O layers. While for the soft  $E_{1u}$  mode, the sliding of the Na layers is about an order stronger than the relative sliding of Co and O layers. Therefore our results follow the trend that displacements modulating the "covalent" bonding produce the largest LO-TO splitting, as being pointed out by Lee et al.<sup>31</sup>.

We also get the Born (dynamical) effective charge tensor. In hexagonal symmetry, it is diagonal and reduces to two values  $Z_{xx} = Z_{yy} = Z_{//}$  and  $Z_{zz} = Z_{\perp}$ . As listed in Table II, these charges show considerable anisotropy in  $\text{NaCoO}_2$ . We notice that  $Z_{\perp}$  is much larger than  $Z_{//}$  for Na, which is consistent with the fact that the LO-TO splitting of the soft in-plane  $E_{1u}$  mode is much smaller than that of the soft out-of-plane  $A_{2u}$  mode, with both modes being dominated by the vibrations of Na. Despite the anisotropy, we define the average effective charge  $\bar{Z}$  as  $\frac{1}{3}\text{Tr}Z$ , which gives about +1, +2 and  $-\frac{3}{2}$  for Na, Co, and O, respectively. The dynamical charges of Co and O are both smaller than their nominal ionic charges. In addition, the static electronic dielectric constants are calculated to be  $\epsilon_{\infty}^{//} = 9.72$ ,  $\epsilon_{\infty}^{\perp} = 4.34$  for geometry *A* and  $\epsilon_{\infty}^{//} = 9.78$ ,  $\epsilon_{\infty}^{\perp} = 4.27$  for geometry *B* respectively.

There are some experimental data on the zone-center phonon frequencies of  $\text{Na}_x\text{CoO}_2$  or  $\text{Na}_x\text{CoO}_2 \cdot y\text{H}_2\text{O}$ . In principle, these frequencies can not be directly compared with our results, since the systems we studied here is  $\text{NaCoO}_2$ . But as we have seen, the Na site occupancy may not affect the frequencies much, especially for the high-frequency in-plane vibration modes. So we also list the experimental Raman and infrared frequencies in Table I for reference. For  $\text{NaCoO}_2$  with only one Na site occupied, symmetry analysis leads to the Raman-active modes  $\Gamma_{\text{Raman}} = A_{1g} + E_{1g} + 2E_{2g}$  and the infrared-active optical phonon modes  $\Gamma_{IR} = 2A_{2u} + 2E_{1u}$ . The experimental Raman frequencies listed in Table I generally agree with our calculated frequencies well. Among the four infrared-active modes, only the frequency of the hard  $E_{1u}$  mode is reported in experiments. The frequency of  $\text{Na}_{0.57}\text{CoO}_2$  reported by Lupi et al.<sup>14</sup> is near our calculated TO frequency of  $E_{1u}$  mode. It is very strange

that infrared spectra by Wang et al.<sup>18</sup> gave four different infrared frequencies for doubly-degenerated in-plane  $E_{1u}$  mode in metallic  $\text{Na}_{0.7}\text{CoO}_2$ , where no LO-TO splitting exists. There should be only two frequencies even considering the partial Na occupation of the  $2b$  and  $2d$  site at the same time. We argue that part of these frequencies may be contributed by defects or grain surface, since the IR reflectivity data are very sensitive to surface treatment. In a word, the IR modes remain to be verified and understood. The peak of optical phonon at  $161.3 \text{ cm}^{-1}$  (20 meV) in neutron inelastic scattering experiment<sup>19</sup> is near the frequency of the soft  $E_{2g}$  mode (mode 1) here.

#### IV. CONCLUSION

In conclusion, we have calculated the lattice dynamics of  $\text{NaCoO}_2$ . Most of the phonon modes are only little affected by the Na site occupancy, and the calculated zone-center phonon frequencies generally agree with those by recent Raman and neutron scattering spectra on corresponding Na de-intercalated and/or hydrated compounds well. Therefore our calculations may also be helpful for understanding the lattice dynamics of the cobalt oxide superconductor. However, to clarify the phonon contribution in the superconductivity requires much further work on the lattice dynamics and electron-phonon interaction of the superconductor itself. Experimental data on infrared-active modes are difficult to compare with our calculated results now. In addition to phonon frequencies, other useful data such as Born effective charges and dielectric constants of  $\text{NaCoO}_2$  are also presented.

#### Acknowledgments

This work is partially supported by the National Project for the Development of Key Fundamental Sciences in China (G1999075305, G2001CB3095), by the National Natural Science Foundation of China (50121202, 20025309, 10074058), by the Foundation of Ministry of Education of China, and by ICTS, CAS.

---

\* Corresponding author. E-mail: jlyang@ustc.edu.cn

- <sup>1</sup> K. Takada, H. Sakurai, E. Takayama-Muromachi, F. Izumi, R. A. Dilanian, and T. Sasaki, *Nature* **422**, 53 (2003)
- <sup>2</sup> J. V. Badding, *Nature Materials* **2**, 208 (2003)
- <sup>3</sup> H. Sakurai, K. Takada, S. Yoshii *et al.*, *Phys. Rev. B* **68**, 312507 (2003)
- <sup>4</sup> K. Ishida, Y. Ihara, Y. Maeno *et al.*, [arXiv:cond-mat/0308506](#).
- <sup>5</sup> W. Higemoto, K. Ohishi, A. Koda *et al.*, [arXiv:cond-mat/0310324](#).
- <sup>6</sup> G. Baskaran, *Phys. Rev. Lett.* **91**, 97003 (2003)
- <sup>7</sup> B. Kumar and B. S. Shastry, *Phys. Rev. B* **68**, 104508 (2003)
- <sup>8</sup> C. Honerkamp, *Phys. Rev. B* **68**, 104510 (2003)
- <sup>9</sup> Q.-H. Wang, D.-H. Lee, and P. A. Lee, [arXiv:cond-mat/0304377](#)
- <sup>10</sup> A. Tanaka and X. Hu, *Phys. Rev. Lett.* **91**, 257006 (2003)
- <sup>11</sup> D. J. Singh, *Phys. Rev. B* **68**, 20503 (2003)
- <sup>12</sup> H. Ikeda, Y. Nisikawa and K. Yamada, [arXiv:cond-mat/0308472](#)
- <sup>13</sup> Y. Tanaka, Y. Yanase, and M. Ogata, [arXiv:cond-mat/0311266](#)
- <sup>14</sup> S. Lupi, M. Ortolani, and P. Calvani, [arXiv:cond-mat/0312512](#)
- <sup>15</sup> C. J. Milne, D. N. Argyriou, A. Chemseddine, N. Aliouane, J. Veira, and D. Alber, [arXiv:cond-mat/0401273](#).
- <sup>16</sup> M. N. Iliev, A. P. Litvinchuk, R. L. Meng *et al.*, *Phys. C* **402**, 239 (2004)
- <sup>17</sup> P. Lemmens, V. Gnezdilov, N. N. Kovaleva *et al.*, [arXiv:cond-mat/0309186](#)
- <sup>18</sup> N. L. Wang, P. Zheng, D. Wu *et al.*, [arXiv:cond-mat/0312630](#)
- <sup>19</sup> A. T. Boothroyd, R. Coldea, D. A. Tennant, [arXiv:cond-mat/0312589](#)
- <sup>20</sup> S. Baroni, S. de Gironcoli, A. Dal Corso, and P. Gianozzi, *Rev. Mod. Phys.* **73**, 515 (2001)
- <sup>21</sup> X. Gonze, *Phys. Rev. B* **55**, 10337 (1997)
- <sup>22</sup> X. Gonze, J.-M. Beuken, R. Caracas *et al.*, *Comput. Mater. Sci.* **25**, 478 (2002)
- <sup>23</sup> M. C. Payne, M. P. Teter, D. C. Allan *et al.*, *Rev. Mod. Phys.* **64**, 1045 (1992)
- <sup>24</sup> X. Gonze, *Phys. Rev. B* **54**, 4383 (1996)
- <sup>25</sup> X. Gonze and C. Lee, *Phys. Rev. B* **55**, 10355 (1997)
- <sup>26</sup> N. Troullier and J. L. Martins, *Phys. Rev. B* **43**, 1993 (1991)
- <sup>27</sup> See the Appendix of S. Goedecker, M. Teter, and J. Hutter, *Phys. Rev. B* **54**, 1703 (1996)
- <sup>28</sup> R. J. Balsys and R. L. Davis, *Solid State Ionics* **93**, 279 (1996)
- <sup>29</sup> J. D. Jorgensen, M. Avdeev, D. G. Hinks *et al.*, [arXiv:cond-mat/0307627](#)

<sup>30</sup> J. W. Lynn, Q. Huang, C. M. Broun *et al.*, arXiv:cond-mat/0307263

<sup>31</sup> K.-W. Lee and W. E. Pickett, Phys. Rev. B **68**, 85308 (2003)



TABLE I: Zone center optical phonon modes of NaCoO<sub>2</sub>. The three groups separated by horizontal lines are Raman-active, infrared-active and silent modes respectively. The involved atoms in each mode and their vibration directions (// for in-plane,  $\perp$  for out-of-plane) are listed. The atomic displacements in parentheses are obtained by dividing the normalized eigenvector components by the square root of the atomic mass, and with the unit of  $10^{-2}$  for convenience of reading. These displacements are only refer to geometry *A*, since they are very similar to those of geometry *B*.  $f^A$  and  $f^B$  stand for calculated frequencies for geometries *A* and *B* respectively, and  $f^{EXP}$  stands for experimental frequencies. For the four infrared-active modes, both the LO and TO frequencies are listed.

Mode	Symmetry	Vibrations			$f^A(\text{cm}^{-1})$	$f^B(\text{cm}^{-1})$	$f^{EXP}(\text{cm}^{-1})$
1	E <sub>2g</sub>	Na <sub>//</sub> (0.34)	O <sub>//</sub> (0.04)		172.9	185.7	
2	E <sub>1g</sub>		O <sub>//</sub> (0.29)		477.1	482.1	458 <sup>a</sup> , 480 <sup>b</sup> , 469 <sup>c</sup>
3	E <sub>2g</sub>	Na <sub>//</sub> (0.05)	O <sub>//</sub> (0.29)		483.7	489.8	494 <sup>a</sup>
4	A <sub>1g</sub>		O $\perp$ (0.29)		608.0	604.6	574 <sup>a</sup> , 598 <sup>b</sup> , 582 <sup>c</sup> , 588 <sup>d</sup>
5	E <sub>1u</sub>	Na <sub>//</sub> (0.31)	Co <sub>//</sub> (0.09)	O <sub>//</sub> (0.05)	201.2	216.5	
					206.3	220.4	
6	A <sub>2u</sub>	Na $\perp$ (0.31)	Co $\perp$ (0.09)	O $\perp$ (0.05)	397.5	337.0	
					418.1	361.6	
7	A <sub>2u</sub>	Na $\perp$ (0.03)	Co $\perp$ (0.12)	O $\perp$ (0.24)	569.8	566.5	
					618.7	615.1	
8	E <sub>1u</sub>	Na <sub>//</sub> (0.03)	Co <sub>//</sub> (0.12)	O <sub>//</sub> (0.24)	586.7	590.0	570 <sup>e</sup> , (505, 530, 560, 575) <sup>f</sup>
					638.5	638.6	
9	E <sub>2u</sub>		Co <sub>//</sub> (0.18)	O <sub>//</sub> (0.16)	88.0	95.2	
10	B <sub>2u</sub>		Co $\perp$ (0.18)	O $\perp$ (0.15)	197.0	172.1	
11	B <sub>1g</sub>	Na $\perp$ (0.33)		O $\perp$ (0.10)	351.7	309.9	
12	E <sub>2u</sub>		Co <sub>//</sub> (0.12)	O <sub>//</sub> (0.24)	582.8	585.6	
13	B <sub>2u</sub>		Co $\perp$ (0.11)	O $\perp$ (0.25)	616.2	610.0	
14	B <sub>1g</sub>	Na $\perp$ (0.11)		O $\perp$ (0.28)	622.4	616.0	

<sup>a</sup> Raman frequency<sup>16</sup> of Na<sub>0.7</sub>CoO<sub>2</sub>.

<sup>b</sup> Raman frequency<sup>17</sup> of Na<sub>x</sub>CoO<sub>2</sub>·*y*H<sub>2</sub>O powder samples with *x* = 0.35.

<sup>c</sup> Raman frequency<sup>17</sup> of Na<sub>0.3</sub>CoO<sub>2</sub>·1.3H<sub>2</sub>O single crystals.

<sup>d</sup> Raman frequency<sup>17</sup> of Na<sub>0.7</sub>CoO<sub>2</sub> single crystals.

<sup>e</sup> Infrared frequency<sup>14</sup> of Na<sub>0.57</sub>CoO<sub>2</sub>.

TABLE II: The Born effective charges of NaCoO<sub>2</sub> atoms. See text for the definition of  $Z_{//}$ ,  $Z_{\perp}$  and  $\bar{Z}$ . Superscripts  $A$  and  $B$  refer to data for geometries  $A$  and  $B$ .

	$Z_{//}$	$Z_{\perp}$	$\bar{Z}$
$Z^A(\text{Na})$	0.87	1.37	1.03
$Z^A(\text{Co})$	2.49	0.87	1.95
$Z^A(\text{O})$	-1.68	-1.12	-1.49
$Z^B(\text{Na})$	0.85	1.40	1.04
$Z^B(\text{Co})$	2.41	0.78	1.86
$Z^B(\text{O})$	-1.63	-1.09	-1.45

FIG. 1: (color online) (a) Structure model of geometry *A*. The smallest balls represent cobalt atoms, and the balls in red bonding to Co are oxygen atoms. Between CoO layers, there exist sodium (big purple ball) layers. (b) Structure model of geometry *B*. (c) Electronic band structure and density of states of NaCoO<sub>2</sub>.

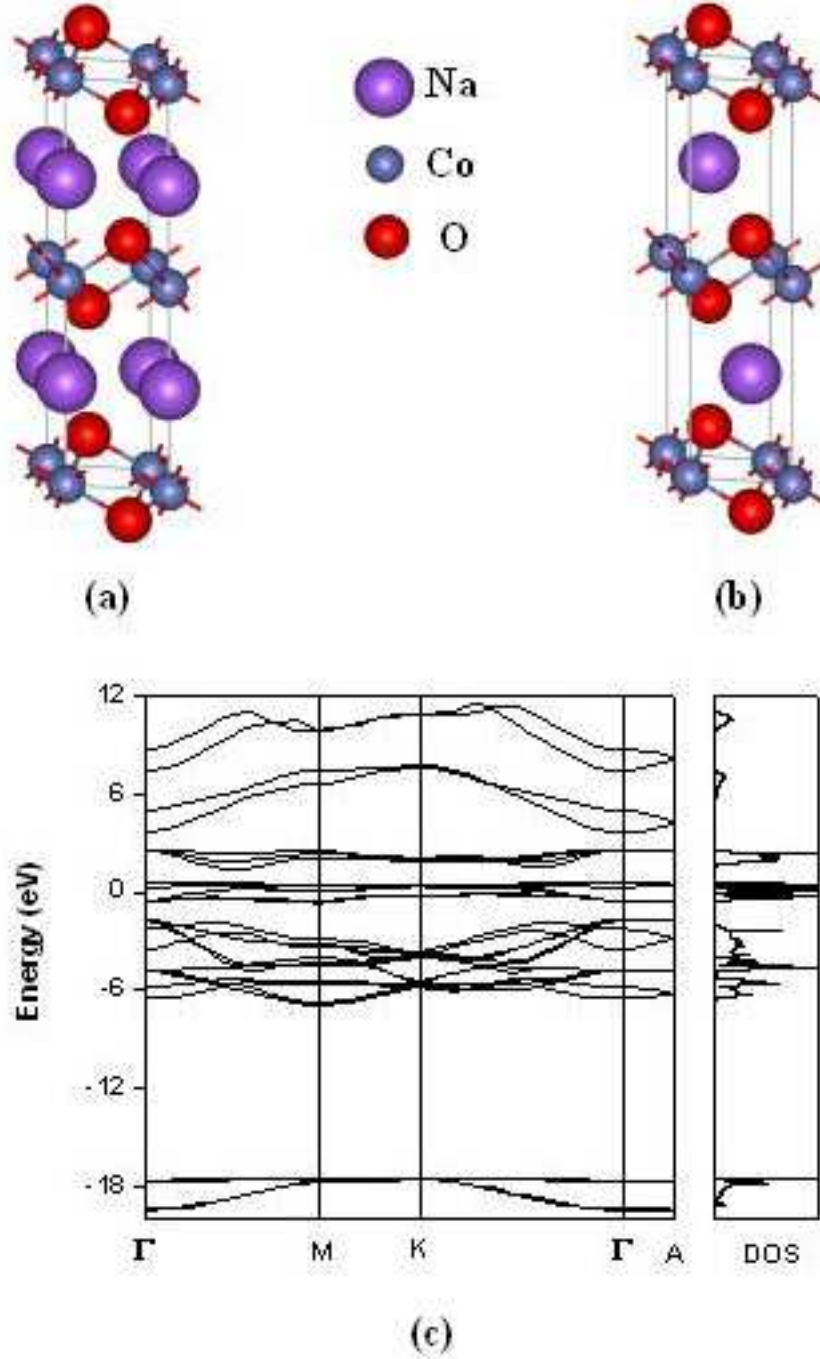


FIG. 2: Phonon band structure and density of states of  $\text{NaCoO}_2$  for (a) geometry  $A$  and (b) geometry  $B$  respectively.

